

Application of liquid phase plasma process to the synthesize ruthenium oxide/activated carbon composite as dielectric material for supercapacitor

Heon Lee¹, Sun-Jae Kim², Kay-Hyeok An³, Jung-Sik Kim⁴, Byung-Hoon Kim⁵, Sang-Chul Jung^{1*}

¹Department of Environmental Engineering, Suncheon National University, 255 Jungang-ro, Suncheon, Jeonnam 540950, Republic of Korea

²Faculty of Nanotechnology and Advanced Materials Engineering, Sejong University, Seoul 143747, Republic of Korea

³Korea Institute of Carbon Convergence Tech., Jeonju 561844, Republic of Korea

⁴Department of Materials Science and Engineering, University of Seoul, 163 Seoulsiripdaero, Dongdaemun-gu, Seoul 130743, Republic of Korea

⁵Department of Dental Materials, Chosun University, 309 Pilmun-daero, Dong-gu, Gwangju 501759, Republic of Korea

*Corresponding author. Tel: (+82) 61-750-3814; E-mail: jsc@sunchon.ac.kr

Received: 24 August 2015, Revised: 03 October 2015 and Accepted: 23 December 2015

ABSTRACT

The ruthenium oxide/activated carbon composite (RCC) were synthesized using an innovative plasma-in-liquid process, which is known as liquid phase plasma (LPP) process. This technique uses a single-step process for the synthesis of metal nanoparticles on supporting materials. LPP process led to simultaneous precipitation of ruthenium and ruthenium oxide nanoparticles on the surface of activated carbon, which is then oxidized to ruthenium oxide during the thermal oxidation process. The specific capacitances of RCC electrodes prepared through the LPP and oxidation process were higher than that of bare AC. The specific capacitance increased with increasing LPP process duration and oxidation treatment. The specific capacitance of ruthenium oxide/carbon composite increased with increasing LPP process duration. The ruthenium oxide/carbon composite prepared through the LPP process and thermal oxidation showed smaller resistances and larger initial resistance slopes than bare activated carbon powder and this effect was intensified by increasing the LPP process duration. The RCC electrodes showed smaller resistances and larger initial resistance slopes than bare AC and this effect was intensified by increasing the LPP process duration and oxidation treatment. Copyright © 2016 VBRI Press.

Keywords: Supercapacitor; RuO₂; activated carbon; specific capacitance; liquid phase plasma.

Introduction

Electrochemical capacitors have been considered as a promising high-power source for digital communication devices and electric vehicles. The advantageous features of electrochemical capacitors are superior rate capability and longer cycle-life compared with modern secondary batteries. Electrochemical capacitors may be classified into two groups, namely, electric double-layer capacitors and pseudo-capacitors [1]. Electric double-layer capacitors (EDLCs) which are generally based on pure graphitic nanostructures including CNTs, graphene, carbon spheres, template derived carbons, activated carbon [2, 3] and pseudo-capacitors which are based on pseudo-capacitive materials like V₂O₅ [4], RuO₂ [5], MnO₂ [6], Co₂O₃ [7], In₂O₃ [8], NiO [9], binary Ni-Co hydroxide [10] which introduce fast surface redox reactions. Among the various metal oxides, ruthenium oxide is a very promising electrode

material for EDLCs, due to its large specific capacitance and good conductivity compared with other oxides [11]. The potential of carbon as an electrode material for supercapacitors has also been recognized due to their unique properties. Therefore, carbon-metal oxide composites are expected to be promising for EDLCs due to their charge-discharge stability.

The preparation of ruthenium oxide/carbon composites has been reported by other workers. Miller *et al.* [12] reported that the specific capacitance of a carbon aerogel is improved more than twice after the addition of hydrous ruthenium oxide by a chemical vapor impregnation method. Wang and Hu [13] prepared RuO₂/activated carbon composites by wet impregnation. Barranco *et al.* [14] reported a capacitance value of about 250 Fg⁻¹ with a composite obtained by repetitive impregnation of amorphous carbon nanofibers with a ruthenium salt solution.

In the present work, ruthenium oxide/activated carbon composite (RCC) electrode materials are prepared by Liquid phase plasma (LPP) method. LPP method is reportedly a useful process to synthesize metal and metal oxide nanoparticles on supporting materials [15]. Metal nanoparticles can be generated rapidly by the LPP process without adding reducing agents [16]. This method uses a one-step process for the synthesis of metal nanoparticles on carbon materials [17]. Hence, in this study, we developed a single-step process for the synthesis of RCC as dielectric material for supercapacitor by LPP reduction process. The effects of plasma discharge conditions are discussed and the resultant products are characterized. The electrochemical capacitance performance of the supercapacitor was evaluated by cyclic voltammetry, electrochemical impedance spectroscopy, and galvanostatic charge/discharge test.

Experimental

Materials and experimental equipment

Ruthenium chloride hydrate ($\text{RuCl}_3 \cdot x\text{H}_2\text{O}$, 45 wt % Ru, Sigma-Aldrich Co.) was used as the precursor for ruthenium nanoparticles. Ruthenium nanoparticles were generated and precipitated in an aqueous solution using the LPP process. Cetyltrimethylammonium bromide (CTAB, $\text{CH}_3(\text{CH}_2)_{15}\text{N}(\text{CH}_3)_3\text{Br}$, Daejung Chemicals & metals Co.) was used as a dispersant in the reactant solution. Supporting material was used as the activated carbon powder (YP-50F, Koraray chemical co.) in this study. The particle size and specific surface area of YP-50F were 5~20 μm and 1,500~1,800 m^2/g , respectively. Reagent-grade chemicals and ultrapure water (Daejung Chemicals & metals Co.) were used in this work. Similar LPP system was used in our previous study to generate nanoparticles dispersed in the solution using the LPP method [17]. Detailed information of the experimental setup can be found in that paper [17]. Pulsed electric discharge was generated by an electrode system in a double annular tube type reactor. Cooling water was circulated through the reactor and the reactant solution temperature was maintained at 298 K. A stirring bar was used in the reactor to maintain the homogeneity of the aqueous solution and the applied voltage, frequency, and pulse width were 250 V, 30 kHz, and 5 μs , respectively.

Preparation of composite

Ruthenium precursor reactant solution was prepared by the following method. $\text{RuCl}_3 \cdot x\text{H}_2\text{O}$ was dissolved in 250 mL of ultrapure water to make a 5 mM aqueous solution. CTAB was added to the solution with a 25 % molar ratio relative to $\text{RuCl}_3 \cdot x\text{H}_2\text{O}$ (1.25 mM). After sufficient stirring, 0.5 g of activated carbon (AC) was added. Ultrasonication for 10 min and stirring for 1 h were performed for complete dispersion of the reaction solution. The LPP reactor was filled with the ruthenium precursor reactant solution and plasma discharge was applied for pre-determined duration (30 min and 60 min) to allow Ru nanoparticles to precipitate on AC surface. After the LPP process, centrifugal process (4,000 rpm) and washing were repeated 5 times to remove unreacted chemicals and surfactant

remaining in the solution from composites. The separated Ru/AC composite was dried at 353 K in a vacuum oven for 48 h. RCC was prepared by oxidizing the dry Ru/AC composite for 2 h in a 423K furnace under an oxygen atmosphere.

Electrochemical test

The electrode of RCC was prepared according to the following steps. The mixture containing 80 wt. % composite and 10 wt. % conducting agent and 10 wt.% binder was well mixed. Super-P conductive carbon black (TIMCAL graphite & carbon com.) was used as the conducting agent. A mixture of PVDF (Polyvinylidene fluoride) and carboxymethyl cellulose (CMC) was used as the binder. The used electrolyte was 6M KOH solution. 150 μm glass felt was used as the separator. The electrochemical behavior of the resulting RCC was also characterized by cyclic voltammetry (CV) and electrochemical impedance spectroscopy (EIS) techniques. The CV measurement was conducted with the actuation voltage of 0.1~0.8 V, the current density of 0.001 A/cm^2 , and the scan rate of 10 mV/s. Impedance was measured using an alternating-current impedance analyzer within the frequency range of 0.1 Hz ~ 300 kHz. Potentiostat (VSP, Princeton applied research) was used to measure electrochemical properties.

Structural characterization

The physical and chemical properties of the RCC synthesized as described above were evaluated using various instruments. Field emission scanning electron microscope (JSM-7100F, JEOL) was used to examine the pattern of dispersion the metal oxide nanoparticles dissipated on the AC powder. The morphology and structure of the RCC was observed using a field emission transmission electron microscope (FETEM, TECNAI-20, FEI). A high resolution FETEM (HR-FETEM, JEM-2100F, JEOL) was used to analyze the crystal structure and lattice of ruthenium oxide nanoparticles. The chemical compositions of the composite were observed using X-photoelectron spectroscopy (XPS, Multilab 2000 system, SSK).

Results and discussion

Characteristics of RCC

Fig. 1 shows the FESEM images of the surface of the RCC prepared by different LPP reaction durations with oxidation treatment: 30 min (a) and 60 min (b). The dots show the mapping images of ruthenium and oxygen, appearing as red and yellow dots, respectively. The number of dots increased with increasing reaction durations of LPP process, indicating that the amount of ruthenium precipitated increased with increasing reaction durations of LPP process. In addition, the dispersion of ruthenium oxide nanoparticles on the AC surface was quite good. This result shows that ruthenium oxide nanoparticles were precipitated uniformly on the surface of AC powders, resulting in successful synthesis of RCC.

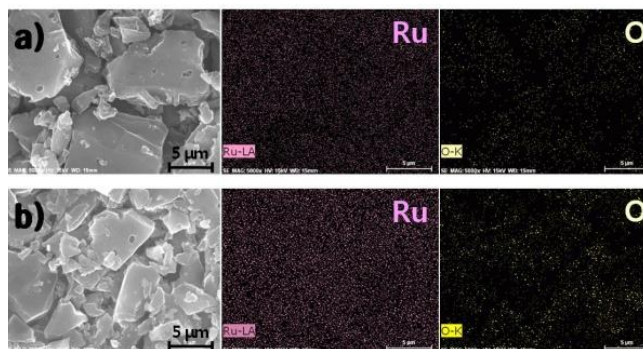


Fig. 1. FESEM images and EDS elemental maps of RCC prepared by different LPP reaction durations with oxidation treatment: 30 min (a) and 60 min (b).

Table 1. Chemical composition of the RCC as a different LPP discharge time and with oxidation treatment.

LPP reaction durations [min]	C		O		Ru	
	Wt %	At %	Wt %	At %	Wt %	At %
Bare AC	96.58	97.41	3.42	2.59	0	0.00
30	82.35	93.17	6.23	5.29	11.42	1.54
30 (oxidation)	80.24	91.47	8.12	6.95	11.64	1.58
60 (oxidation)	75.09	89.22	9.67	8.63	15.24	2.15

The chemical compositions of the RCC synthesized with different LPP reaction durations and oxidation treatment, analyzed using EDX spectrum, are summarized in **Table 1**. The bare AC consisted of 97.41 % of carbon and 2.59 % of oxygen, in atomic %. **Table 1** also shows the composition of the composite prepared through 30-min LPP process only (without oxidation). The oxygen quantity of this composite was 5.29 At %, which was higher than that of bare AC (2.59 At %) but lower than that of the composite prepared through 30 min LPP process and oxidation (6.95 At %). This result is attributed to the simultaneous precipitation of ruthenium metal and ruthenium oxide onto AC during the LPP process. In our previous studies [15-17], both metal nanoparticles and metal oxide nanoparticles were produced during the synthesis of nanoparticles using LPP process. In the LPP region, various oxidative species ($\text{OH}\cdot$, $\text{O}\cdot$, $^1\text{O}_2$, HO_2 , O_2^- , H_2O_2 , O_3 , etc.), as well as electrons, are produced at high temperature because of some metal nanoparticles are oxidized into metal oxide nanoparticles by these oxidative species. For the RCC that passed through the oxidation process, the quantity of Ru precipitation increased with increasing LPP process duration, which is in good agreement with the result shown in **Fig. 1**. The oxygen quantity in the RCC also increased with increasing LPP process duration, which is attributed to the oxidation of ruthenium metal precipitated.

Fig. 2 shows the FETEM image of RCC prepared by different LPP reaction durations with oxidation treatment. Spherical shaped ruthenium oxide nanoparticles of about 30~50 nm size were observed after 30 min LPP reaction time (a) and about 40~90 nm in size were mainly produced after 60 min. Both the particle size and the particle number were observed to increase with the length of LPP reaction durations in this study. As well as, the number of ruthenium oxide nanoparticles generated increased with increasing

initial ruthenium precursor concentration in this preliminary experiment. This study was aimed at dispersing ruthenium oxide nanoparticles as small as possible evenly on the surface of AC. Therefore, a process condition was chosen so that spherical ruthenium oxide nanoparticles smaller than 100 nm could be produced.

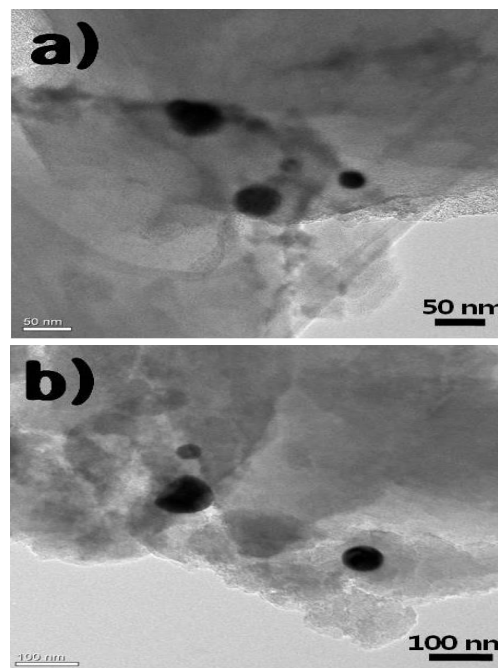


Fig. 2. FETEM image of RCC prepared by different LPP reaction durations; 30 min (a) and 60 min (b).

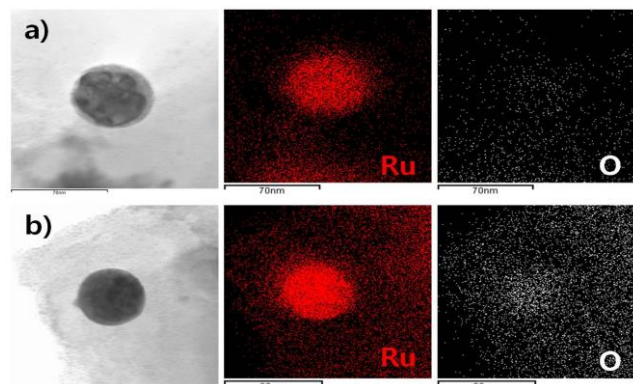


Fig. 3. HR-TEM image and element mapped of ruthenium oxide nanoparticles on the AC surface as a function of a) as precipitation and b) with oxidation treatment.

Fig. 3 shows the HR-FETEM images of ruthenium oxide nanoparticles on the AC, and the mapping images of ruthenium element (red dot) and oxygen element (white dot) obtained 30 min LPP reaction time with un-oxidation (a) and oxidation (b). Spherical shaped nanoparticles like the ones shown in **Fig. 2** were observed for both oxidation conditions. The oxygen element mapping image showed that oxidation of nanoparticle (b) led to higher oxygen element than un-oxidation of nanoparticle (a), agreeing with the results of **Table 1**. This result shows that ruthenium nanoparticles were oxidation on the surface of AC powders, resulting in successful synthesis of RCC.

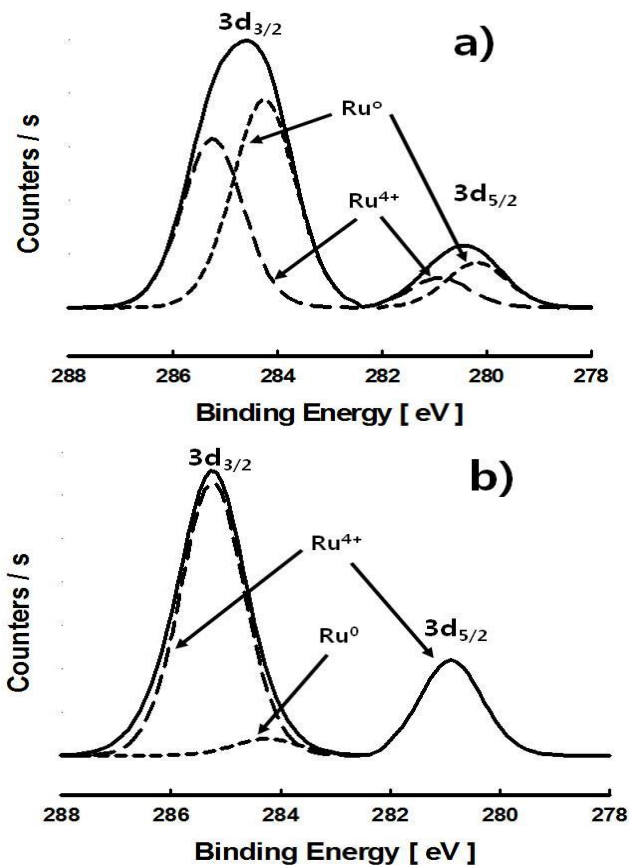


Fig. 4. High resolution XPS spectra for the Ru3d regions of RCC prepared by LPP process.

X-photoelectron spectroscopy is currently the most heavily used analytical techniques to obtain information about composition and chemical information at solid surfaces. In XPS full range spectrum of RCC prepared by 30 min LPP process without oxidation, the peaks for carbon C1s and Ru3d were observed at 284 and the oxygen O1s were observed at 530 eV. The Ru3p_{3/2} and Ru3p_{1/2} peaks appeared at 462 and 484 eV, respectively. This result is attributed, as was pointed out in **Table 1**, to the simultaneous precipitation of ruthenium metal and ruthenium oxide onto AC during the LPP process. Ruthenium metal particles are first formed due to the reduction of ruthenium ions by electrons during the LPP process and then ruthenium oxide is produced by the oxidation of ruthenium metal in acidic reaction solution, which resulted in enhanced O1s peak of ruthenium oxide/AC composite. In this work, the composites produced through the LPP process were oxidized at 423 K under an oxygen atmosphere to synthesize RCC. To investigate the effects of LPP reactions and oxidation on the chemical structure of ruthenium particles produced, XPS analysis was carried out. **Fig. 4** compares the narrow-range XPS spectra of Ru element of the RCC prepared by 30-min LPP process only (a) and that of RCC prepared by 30-min LPP process with thermal oxidation (b). Ruthenium particles are known to exist in the forms of Ru⁰ and RuO₂ [18-20]. The un-oxidation composite showed Ru⁰ (280.2 and 284.2 eV) and Ru⁴⁺ (280.9 and 285.36 eV) peaks (**Fig. 4a**). This indicates the coexistence of ruthenium metal and ruthenium oxide particles, being in good agreement with

the results shown in **Table 1**. On the other hand, the RCC show very small Ru⁰ peak (**Fig. 4b**). These results indicate that ruthenium metal was oxidized by thermal treatment.

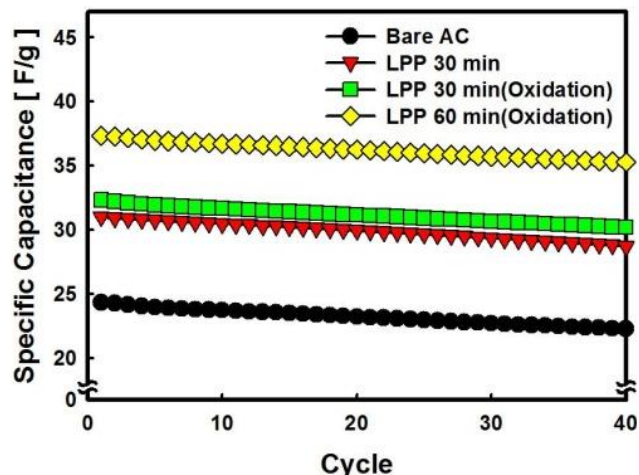


Fig. 5. Specific capacitance of RCC prepared by different LPP reaction durations and oxidation treatment.

Electrochemical measurements of RCC electrode

The electrochemical stability of the RCC electrode prepared by different LPP reaction durations and oxidation treatment was examined by charge–discharge cycling and the results are shown in **Fig. 5**. Bare AC (YP-50) showed the lowest initial specific capacitance of 24.33 F/g at the first measurement but at the 40th cycle the specific capacitance was decreased by 8.5 % to 22.28 F/g. The RCC prepared through only 30-min LPP reaction duration showed initial specific capacitance (31.00 F/g). The initial specific capacitance values of the RCC prepared through LPP process for 30 min and 60 min and oxidation treatment were 32.33 and 37.33 F/g, respectively, being all higher than that of bare AC. The RCC also showed small capacitance loss by repeated charge/discharge. The absorption/desorption of the electrolyte ions onto the surface of the Ru ion may add to the capacitance through pseudo-capacitive and electrochemical reactions [21].

Fig. 6a compares the current-voltage curves, plotted using the cyclic voltammetry measurement with a potential scan rate of 10 mV/s in the range of 0.1–0.8 V, of RCC prepared with different LPP reaction durations and oxidation treatment. All the RCC electrodes tested showed ideal rectangular CV curves of electric double-layer capacitor. Although it is difficult to distinguish the CV curves shown in **Fig. 6a**, the RCC prepared through only 30-min LPP reaction duration showed the worst charge–discharge characteristic, whereas the charge–discharge characteristic of RCC became better with increasing LPP process duration and oxidation treatment. The CV curve provides the measure of capacitors charge response with charging voltage and hence can be used to evaluate the capacitance.

The pseudo-capacitance of transition metal oxides have been attributed to redox transition of species at various oxidation states [22]. The proposed redox reaction for the ruthenium oxide electrode showing capacitance will be as follows:



It is presumed that the RCC has enhanced charge storage and improved C-V characteristics due to the existence of ruthenium oxide produced by thermal treatment.

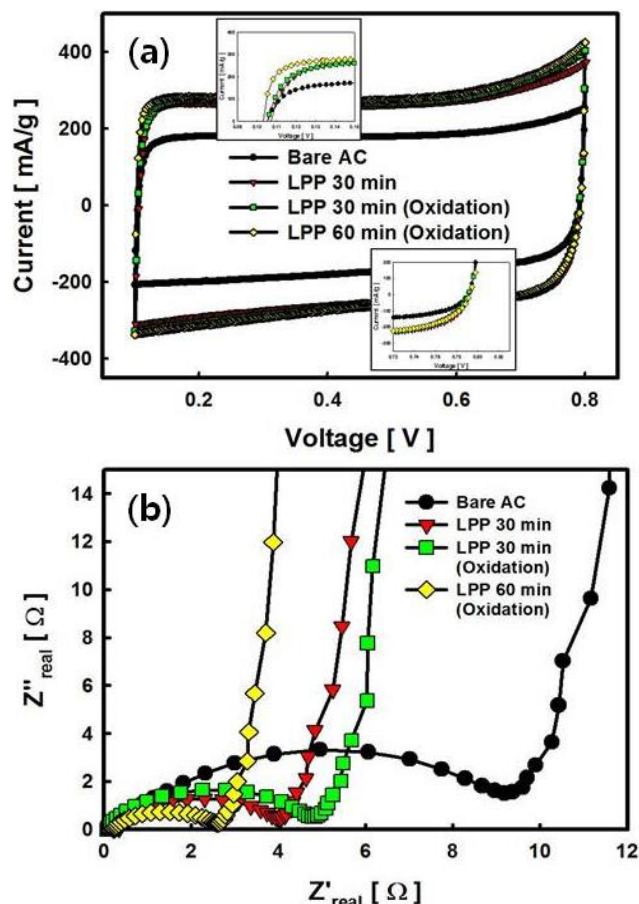


Fig. 6. C-V curves(a) and nyquist plot(b) of RCC prepared by LPP process as a function of different LPP reaction durations and oxidation conditions.

Fig. 6b compares the Nyquist plots, which shows the impedances of the coin cell batteries made of bare AC and RCC electrode prepared with different LPP reaction durations and oxidation conditions. Half circle-shaped Nyquist plot, representing the resistance between electrolyte and electrode, indicates a decline of the capacitor quality. In the high frequency region, the size of semicircle indicates the magnitude of the resistance between electrolyte and anode material. The semicircle size is called equivalent series resistance (ESR). A higher ESR indicates a higher resistance and more difficult charge transport. The ESR of the anode material used in this study (YP-50F) was 9.18Ω , whereas that of RCC prepared through only 30-min LPP reaction duration was 4.01Ω . The precipitation of ruthenium oxide particles reduced the resistance because the resistance of ruthenium is smaller than that of AC. The ESR levels of the RCC prepared by LPP reaction duration of 30 min and 60 min with oxidation treatment were 4.77Ω and 2.59Ω , respectively, decreasing with increasing reaction duration due to increased

precipitation of ruthenium oxide. In the lower frequency region, the slope indicates the capacitive behavior. An infinity slope represents pure capacitive behavior. The slope of bare AC (YP-50F) used in this study was 7.64. LPP process for 30 min (without oxidation) slightly increased it to 8.67, whereas oxidation treatment on top of LPP reaction for 30 min and 60 min increased it to 8.95 and 9.09, respectively, indicating that the diffusion rate of ions inside the electrode structure is increased by ruthenium oxide formed during the LPP reaction and oxidation treatment.

Conclusion

Ruthenium oxide/activated carbon composite electrodes for supercapacitor were prepared by the LPP process. Ruthenium oxide nanoparticles were evenly dispersed on the surface of AC and that the quantity of Ru precipitated increased with increasing LPP reaction duration. EDX and XPS analyses showed that LPP process led to simultaneous precipitation of ruthenium and ruthenium oxide nanoparticles on the surface of AC powder, which is then oxidized to ruthenium oxide during the thermal oxidation process. HR-FETEM observation showed that the average size of the spherical ruthenium oxide nanoparticles precipitated evenly on the AC surface was about 30~90 nm. The specific capacitances of ruthenium oxide/carbon composite electrodes prepared through the LPP and oxidation process were higher than that of bare AC. The specific capacitance increased with increasing LPP process duration and oxidation treatment. The ruthenium oxide/carbon composite electrodes showed smaller resistances and larger initial resistance slopes than bare AC. This effect was intensified by increasing the LPP process duration and oxidation treatment.

Acknowledgements

This work was supported by the Technology Innovation Program (10050391, Development of carbon-based electrode materials with $2,000\text{m}^2/\text{g}$ grade surface area for energy storage device) funded By the Ministry of Trade, industry & Energy (MI, Korea).

Author contributions

Conceived the plan: S J; Performed the experiments: H L; Data analysis: S K, K A, J K; Wrote the paper: S J. Authors have no competing financial interests.

Reference

- Conway, B. E.; *J. Electrochem. Soc.* **1991**, *138*, 1539.
DOI: [10.1149/1.2085829](https://doi.org/10.1149/1.2085829)
- David, Pech, D.; Brunet, M.; Durou, H.; Huang, P.; Mochalin, V.; Gogotsi, Y.; Taberna, P. L.; Simon, P.; *Nat. Nanotechnol.* **2010**, *5*, 651.
DOI: [10.1038/nnano.2010.162](https://doi.org/10.1038/nnano.2010.162)
- Chmiola, J.; Largeot, C.; Taberna, P. L.; Simon, P.; Gogotsi, Y.; *Science* **2010**, *328*, 480.
DOI: [10.1126/science.1184126](https://doi.org/10.1126/science.1184126)
- Perera, S. D.; Patel, B.; Nijem, N.; Roodenko, K.; Seitz, O.; Ferraris, J. P.; Chabal, Y. J.; Balkus Jr., K. J.; *Adv. Energy Mater.* **2011**, *1*, 936.
DOI: [10.1002/aenm.201100221](https://doi.org/10.1002/aenm.201100221)
- Jang, J. H.; Han, S.; Hyeon, T.; Oh, S. M.; *J. Power Sources* **2003**, *123*, 79.
DOI: [10.1016/S0378-7753\(03\)00459-2](https://doi.org/10.1016/S0378-7753(03)00459-2)
- Hou, Y.; Chen, L.; Liu, P.; Kang, J.; Fujita, T.; Chen, M.; *J. Mater. Chem. A* **2014**, *2*, 10910.
DOI: [10.1039/C4TA00969J](https://doi.org/10.1039/C4TA00969J)


7. Dong, X. C.; Xu, H.; Wang, X. W.; Huang, Y. X.; Chan-Park, M. B.; Zhang, H.; *ACS Nano* **2012**, *6*, 3206.
DOI: [10.1021/nn300097q](https://doi.org/10.1021/nn300097q)
8. Bastakoti, B. P.; Oveisi, H.; Hu, C. C.; Wu, K. C. W.; Suzuki, N.; Takai, K.; Kamachi, Imura, M.; Yamauchi, Y.; *Eur. J. Inorg. Chem.* **2013**, *2013*, 1109.
DOI: [10.1002/ejic.201201311](https://doi.org/10.1002/ejic.201201311)
9. Nam, K. W.; Kim, K. B.; *J. Electrochem. Soc.* **2002**, *149*, A346.
DOI: [10.1149/1.1449951](https://doi.org/10.1149/1.1449951)
10. Bastakoti, B. P.; Kamachi, Y.; Huang, H. S.; Chen, L. C.; Wu, K. C. W.; Yamauchi, Y.; *Eur. J. Inorg. Chem.* **2013**, *2013*, 39.
DOI: [10.1002/ejic.201200939](https://doi.org/10.1002/ejic.201200939)
11. Zheng, J. P.; Jow, T. R.; *J. Electrochem. Soc.* **1995**, *142*, L6.
DOI: [10.1149/1.2043984](https://doi.org/10.1149/1.2043984)
12. Miller, J. M.; Dunn, B.; Tran, T. D.; Pekala, R. W.; *J. Electrochem. Soc.* **1997**, *144*, L309.
DOI: [10.1149/1.1838142](https://doi.org/10.1149/1.1838142)
13. Wang, C. C.; Hu, C. C.; *Mater. Chem. Phys.* **2004**, *83*, 289.
DOI: [10.1016/j.matchemphys.2003.09.047](https://doi.org/10.1016/j.matchemphys.2003.09.047)
14. Barranco, V.; Pico, F.; Ibañez, J.; Lillo-Rodenas, M. A.; Linares-Solano, A.; Kimura, M.; Oya, A.; Rojas, R. M.; Amarilla, J. M.; Rojo, J. M.; *Electrochim Acta* **2009**, *54*, 7452.
DOI: [10.1016/j.electacta.2009.07.080](https://doi.org/10.1016/j.electacta.2009.07.080)
15. Lee, H.; Park, S. H.; Kim, S. J.; Park, Y. K.; Kim, B. H.; Jung, S. C.; *Microelectron. Eng.* **2014**, *126*, 153.
DOI: [10.1016/j.mee.2014.07.014](https://doi.org/10.1016/j.mee.2014.07.014)
16. Kim, S. C.; Kim, B. H.; Kim, S. J.; Lee, Y. S.; Kim, H. G.; Lee, H.; Park, S. H.; Jung, S. C.; *J. Nanosci. Nanotechnol.* **2015**, *15*, 228.
DOI: [10.1166/jnn.2015.8340](https://doi.org/10.1166/jnn.2015.8340)
17. Lee, H.; Park, S. H.; Kim, S. J.; Park, Y. K.; Kim, B. J.; An, K. H.; Ki, S. J.; Jung, S. C.; *Int. J. Hydrogen Energ.* **2015**, *40*, 754.
DOI: [10.1016/j.ijhydene.2014.08.085](https://doi.org/10.1016/j.ijhydene.2014.08.085)
18. Song, Y.; Chen, Y.; Chi, Y.; Liu, C.; Ching, W.; Kai, J.; Chen, R.; Huang, Y.; Carty, A. J.; *Chem. Vap. Deposition*, **2003**, *9*, 162.
DOI: [10.1002/cvde.200306242](https://doi.org/10.1002/cvde.200306242)
19. Hu, C. C.; Chang, K. H.; Lin, M. C.; Wu, Y. T. *Nano Letters* **2006**, *6*, 2690.
DOI: [10.1021/nl061576a](https://doi.org/10.1021/nl061576a)
20. Long, J. W.; Sassin, M. B.; Fischer, A. E.; Rolison, D. R.; Mansour, A. N.; Johnson, V. S.; Stallworth, P. E.; Greenbaum, S. G. *J. Phys. Chem. C* **2009**, *113*, 17595.
DOI: [10.1021/jp9070696](https://doi.org/10.1021/jp9070696)
21. Ramani, M.; Haran, B. S.; White, R. E.; Popov, B. N.; Arsov, L. *J. Power Sources*, **2001**, *93*, 209.
DOI: [10.1016/S0378-7753\(00\)00575-9](https://doi.org/10.1016/S0378-7753(00)00575-9)
22. Terasawa, N.; Mukai, K.; Yamato, K.; Asaka, K. *Sens. Actuators, B*, **2012**, *174*, 217.
DOI: [10.1016/j.snb.2012.08.055](https://doi.org/10.1016/j.snb.2012.08.055)

Advanced Materials Letters

Copyright © 2016 VBRI Press AB, Sweden
www.vbripress.com/aml and www.amlett.com

Publish your article in this journal

Advanced Materials Letters is an official international journal of International Association of Advanced Materials (IAAM, www.iaamonline.org) published monthly by VBRI Press AB from Sweden. The journal is intended to provide high-quality peer-review articles in the fascinating field of materials science and technology particularly in the area of structure, synthesis and processing, characterisation, advanced-state properties and applications of materials. All published articles are indexed in various databases and are available download for free. The manuscript management system is completely electronic and has fast and fair peer-review process. The journal includes review article, research article, notes, letter to editor and short communications.



A Monthly Journal

